Massively Parallel Large-Scale Multi-Model Simulation of Tumour Development Including Treatments

M. Berghoff, J. Rosenbauer, A. Schug

published in

NIC Symposium 2020
M. Müller, K. Binder, A. Trautmann (Editors)

Forschungszentrum Jülich GmbH,
John von Neumann Institute for Computing (NIC),
Schriften des Forschungszentrums Jülich, NIC Series, Vol. 50,
ISBN 978-3-95806-443-0, pp. 63.
http://hdl.handle.net/2128/24435

Massively Parallel Large-Scale Multi-Model Simulation of Tumour Development Including Treatments

Marco Berghoff[1], **Jakob Rosenbauer**[2], **and Alexander Schug**[2]

[1] Karlsruhe Institute of Technology, Karlsruhe, Germany
E-mail: marco.berghoff@kit.edu

[2] John von Neumann Institute for Computing and Jülich Supercomputing Centre, Institute for Advanced Simulation, Forschungszentrum Jülich, 52425 Jülich, Germany
E-mail: al.schug@fz-juelich.de

The temporal and spatial resolution in the microscopy of tissues has increased significantly within the last years, yielding new insights into the dynamics of tissue development and the role of single cells within it. Still, the theoretical description of the connection of single cell processes to macroscopic tissue reorganisations is lacking. Especially in tumour development, single cells play a crucial role in the advance of tumour properties. We developed a simulation framework that can model tissue development up to the centimetre scale with micrometre resolution of single cells. Through parallelisation, it enables the efficient use of high-performance computing systems, therefore enabling detailed simulations on 10.000s of cores. Our generalised tumour model respects adhesion driven cell migration, cell-to-cell signalling, and mutation-driven tumour heterogeneity. We scan the response of the tumour development depending on division inhibiting substances such as cytostatic agents. Furthermore, we are investigating the interaction with radiotherapy to find a suitable therapy plan. Currently, the emergence of ever-more-powerful experimental techniques such as light sheet microscopy already offers unprecedented subcellular insight into tissue dynamics. Combined with powerful machine learning techniques, such large data sets (TB's +) can be effectively evaluated promising realistic parameters for our simulations for topics ranging from cancer development to embryogenesis or morphogenesis with considerable impact both for basic science and applied biomedical fields.

1 Model

Especially in tumour development, the behaviour of single cells plays a significant role in the tumour characteristics and progression. This microscale can be essential for the emergence of macroscopic tumour growth and the emergine tumour properties. Simultaneously, tumours that are clinically relevant consist of millions of cells thereby setting the upper border for the simulated spatial resolution.

Over the last decade the theoretical and computational description of cell and tissue dynamics and processes has developed to be a valuable tool to complement experiments.[1–4] Models are applied in embryogenesis and tissue patterning[5–7] as well as tumour development[8–11] and treatment.[12, 13] At the same time the experimental accessibility of entire tissues and its properties has greatly increased through modern microscopic techniques such as light-sheet microscopy[14] and confocal microscopy[15] as well as CRISPR techniques.[16] The combination of contemporary experimental techniques with the recent advances in machine learning enables the analysis of large datasets in various spacial regimes[17–19] and translating the properties into model parameters.[20, 21]

However, the computational models that are published so far either concentrate on the detailed descriptions on a small number of cells or a coarse grained description of cells for

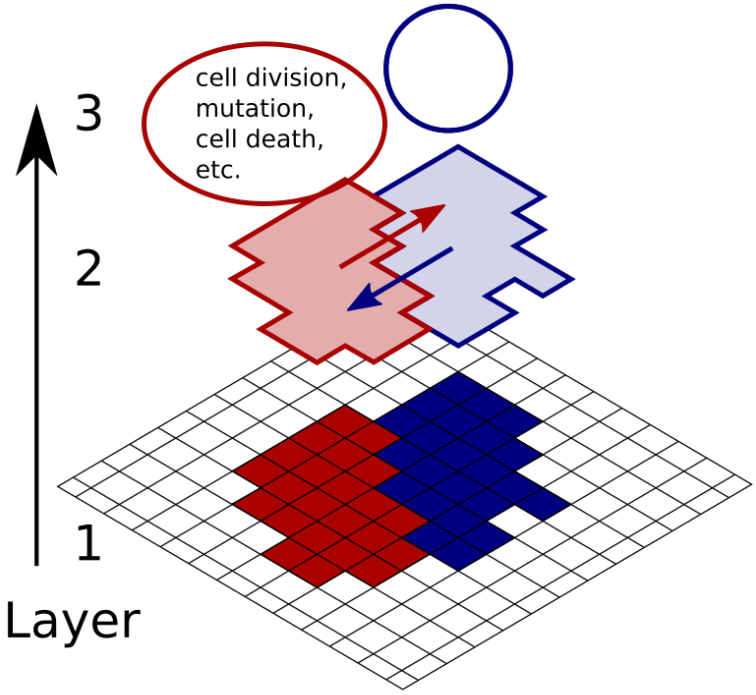

Figure 1. A two-dimensional schematic diagram shows the three different model levels. The lowest layer, the microscale, contains a grid based cellular Potts model to model tissue dynamics. On the highest layer, the macroscale, an agent-based model is acting. In between, on the mesoscale, the transport of signals is processed.

larger tissues. To be able to simulate both, the individual cellular geometry as well as the macroscopic tumour a high degree of parallelism is needed, which we introduce with our model. We use the massively parallel NAStJA framework[22, 23] to implement a multi-model solver with a cell-geometric resolution for the simulation of tissue growth in general and cancer in particular.

The model consists of three layers to accommodate for this large spatial range. On the microscale layer a cellular Potts model simulates adhesion driven cell movements, cell dynamics and cell-to-cell interactions. On the most coarse layer, an agent-based model is used, where each cell corresponds to one agent. On this macroscale layer, the signals are processed, and cell death and cell division, including mutations, are simulated. Another model layer lies between these two scales. It represents the mesoscale and ensures signal diffusion through the surfaces of the cells. Fig. 1 shows an overview of the different model levels. Following the three model layers are described in detail. Each model layer acts on its specific scale.

Microscale The model is based on a regular rectangular grid. Each voxel has an integer number that represents the cell ID. All voxels with the same cell ID are assigned to a biological cell. The cellular Potts model is a Monte Carlo method:[24] The system evolves

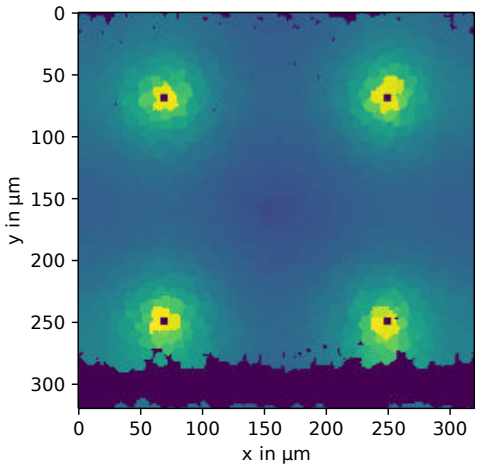

Figure 2. Diffusion of the nutrient signal, the four black squares are blood vessels, that supply the nutrient. Yellow cells have high nutrient concentrations and blue ones low.

under random changes of nearest-neighbour voxels at cell surfaces. These changes are accepted according to a Metropolis acceptance criterion. A Hamiltonian defines the energy of the system. It is the sum of several energy functions:

$$H_{\text{CPM}} = \sum_{i\in\Omega}\sum_{j\in N(i)} J_{\tau(\varsigma_i),\tau(\varsigma_j')}(1-\delta(\varsigma_i,\varsigma_j')) + \lambda_{\text{v}}\sum_{i\in\Omega}\left(v(\varsigma_i)-V(\tau(\varsigma_i))\right)^2 + \lambda_{\text{s}}\sum_{i\in\Omega}\left(s(\varsigma_i)-S(\tau(\varsigma_i))\right)^2 \tag{1}$$

Here, the first sum corresponds to the cell adhesion, the second to the volume, and the last corresponds to the surface of individual cells. While the system evolves, each cell has a target volume V and a target surface S. Possible Monte-Carlo steps are nearest neighbour interactions of adjacent grid points, leading to small changes on the cells surface geometries. Therefore the Monte-Carlo propagation of the system corresponds to a time step, that can be mapped to a physical time. This is modelled by the energy minimisation of the whole non-steady-state system. The implementation of the Hamiltonian is versatile so that the single terms of the energy can be replaced by other terms, *e. g.* different kinds of volume estimations. Besides, the energy sum can be extended by several other terms, *e. g.* adaption to a local or global potential (introduced by the Glazier-Graner-Hogeweg model[25]).

Mesoscale On this scale, the diffusion of signals is simulated. Signals can be among others oxygen, nutrients or therapeutic drugs. Based on the common surface with neighbouring cells, the signals diffuse from one cell to the other, see Fig. 2.

Macroscale At the most coarse level, each cell is assigned to an agent. The individual agents are then responsible for signal processing, *e. g.* usage of nutrient, producing of signals. These agents also control the cell cycle of the individual cell. Events such as cell death and cell division can be induced depending on internal and external parameters of the cell, such as the signal concentration, cell age and therapeutic agents. A set of cell types is defined, each cell type has a specific set of parameters, determining the behaviour of the individual cell belonging to that cell type. Parameters of a single cell type include micro, meso, and macroscale parameters such as the target volume and surface V, S, as well as division rate p_{div} and diffusion constants D, *etc.* After cell division, cells may mutate, depending on external parameters as well as predefined rates. A mutation alters the cell properties, which is implemented by a change of the cell type with defined transition rates between each cell type. The agents take the domain distribution into account and can thus perform cell division correctly, even if the geometric resolution of the cell is distributed over several processes.

2 Scaling

The code is implemented within the NAStJA framework so that it can benefit directly from the excellent scalability. The domain is divided into subdomains and distributed to the MPI ranks. Each MPI rank then holds a block containing the field on the microscale with the cell IDs and additional cell data, which are held for the higher scales, per cell. After each calculation sweep, a halo exchange to the first 26 neighbour blocks is used for the field of cell IDs. Initially, the additional data of the cells must be exchanged globally, since it is not known where the cells are located. That would result in a poorly-scaling collective communication. Domain knowledge about the size of the cells gives the possibility to chose the size of the blocks at least three-fold larger compared to the cells. With this, it can be ensured that a cell is never distributed over more than eight blocks, *i. e.* two per dimension, at the same time, compare Fig. 3. With this knowledge, it can be ensured that

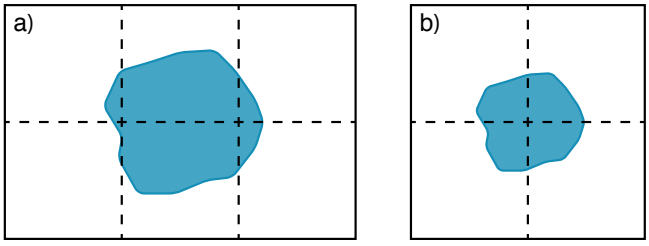

Figure 3. A cell (blue) is distributed to several blocks. (a) shows an inadequate distribution and (b) shows an allowed distribution.

the bookkeeping of the additional data can be handled by local communications to the next 26 neighbours. The efficiency of this exchange is excellent, as shown in Fig. 4(a). Fig. 4(b) right shows an efficiency of $> 80\,\%$ for blocks with an edge length of 100 and even an efficiency of $> 90\,\%$ for an edge length of 200. This result was measured on JURECA with up to 256 nodes corresponding to 6144 processes.

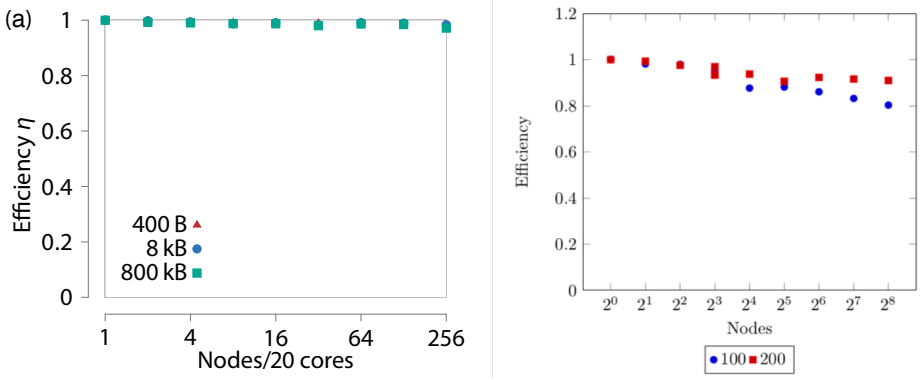

Figure 4. (a) The efficiency of the data exchange on ForHLR II and (b) the efficiency for the whole simulation on JURECA, using up to 256 nodes with 24 cores each. It is shown for a subdomain distribution with a block edge length of 100 and 200.

3 Application

To validate our model implementation we model adhesion driven cell sorting, as it was described in two dimensions in the initial paper of Graner and Glazier.[24] We use a three-dimensional spherical arrangement of randomly mixed cells. Two cell types with differential adhesion are introduced and randomly assigned to the cells. The cell-to-cell adhesion of cells belonging to the same cell type is larger than the adhesion between different cell types. This leads to a demixing of the cell types and formation of clusters as can be seen in Fig. 5. Reproducing the expected behaviour and showing accordance of our three-dimensional implementation with the initial two-dimensional model.

We apply the model on the growth of heterogeneous tumours. A domain is filled with non-dividing tissue cells, that make up the surrounding in which the tumour develops. Each cell has a volume of about 1000 voxels. A network of blood vessels spanning the entire domain is introduced and serves as the source of nutrients and medication. A small nucleus of cancer cells is placed in the centre of the simulated tissue. The cancerous cells proliferate and develop a tumour through cell division. Cells divide when abundant nutrition is present, leading to an increased growth adjacent to blood vessels and hypoxic regions where is a sparse vascularisation. In hypoxic regions cell-division is down-regulated while cell death is up-regulated leading to a negative growth.

Tumour cells can mutate after cell division into one of the 30 predefined cell types. Each cell type provides different properties and therefore enhances or hinders the propagation of the tumour depending on the localisation within the tissue. A heterogeneous tumour forms with its composition of sub-populations of different cell types depending on external conditions. Tumour heterogeneity is a pivotal property of tumours since it enables the specialisation and adaptation of the tumour and leads to complications in tumour treatment. In order to recreate those properties observed *in vivo*, two different treatment types are incorporated into our model:

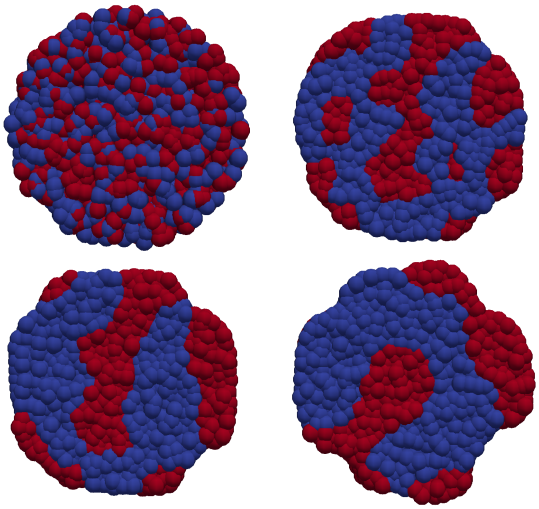

Figure 5. Adhesion driven cell sorting. Time evolution of a two dimensional slice of the three dimensional simulation. The colours represent different cell types. Times are initial condition and after $20 \cdot 10^6$, $45 \cdot 10^6$ and $110 \cdot 10^6$ Monte Carlo sweeps.

Chemotherapy is realised by the introduction of a cytostatic drug that down-regulates cell-division. The drug is distributed via the blood vessels. Since only cell-division is affected by the drug, the tumour shrinks due to cell-death still being present.

Radiation therapy reduces the division rate globally and immediately initiates the cell-death of a fraction of the tumour cells.

With these mechanisms established, treatments can then be optimised for different tumours. This is done by scanning different treatment protocols such as single pulse, multiple pulses and combinations of chemo- and radiotherapy. The effect on the total tumour volume as well as the tumour composition is analysed and can give valuable information about the generation of heterogeneity development of a tumour. This is illustrated in Fig. 6, where chemo- or radiotherapy individually do not lead to success, but a combination does. Multiple pulses of chemo- or radiotherapy lead to the development of a nearly homogeneous tumour, with one dominating cell type.

4 Conclusion

We were able to show that with a highly parallel framework and a multiscale model, the development of tumours can be simulated. We are able to simulate heterogeneous tumour growth and development in a domain measuring $1000 \times 1000 \times 1000$ voxels corresponding to a tissue of $1\,\mathrm{mm}^3$. The cell-geometric resolution was chosen to reproduce the tumour characteristics, which depend significantly on the adhesion between the individual cells. Besides, we have shown that different treatments can be performed. Thus, many different

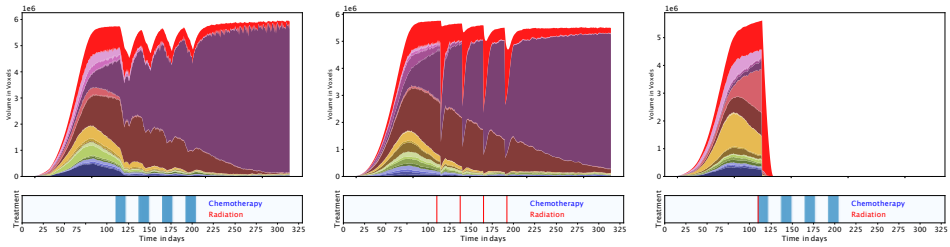

Figure 6. Change of volume of the tumour under different treatment plans of chemotherapy and radiation, single or in combination. The colours represent different cell types.

treatment plans can be simulated before the treatment on the patient, and then the best one can be selected for the patient.

Due to the flexibility of the framework, the model can be easily extended, and further effects can be considered, in future versions.

Acknowledgements

The authors gratefully acknowledge the computing time granted by the John von Neumann Institute for Computing (NIC) and provided on the supercomputer JURECA[26] at Jülich Supercomputing Centre (JSC). This work was partially supported by the Helmholtz Analytics Framework of the Helmholtz Association under project number ZT-I-0003.

References

1. L. M. Loew and J. C. Schaff, *The Virtual Cell: a software environment for computational cell biology*, TRENDS in Biotechnology **19**, 401–406, 2001.
2. M. H. Swat, G. L. Thomas, J. M. Belmonte, A. Shirinifard, D. Hmeljak, and J. A. Glazier, *Multi-scale modeling of tissues using compucell3d*, in Methods in cell biology **110**, A. R. Asthagiri and A. P. Arkin (Editors), Elsevier, 325–366, 2012.
3. A. Ghaffarizadeh, R. Heiland, S. H. Friedman, S. M. Mumenthaler, and P. Macklin, *PhysiCell: An open source physics-based cell simulator for 3-D multicellular systems*, PLoS computational biology **14**, e1005991, 2018.
4. P. M. Altrock, L. L. Liu, and F. Michor, *The mathematics of cancer: integrating quantitative models*, Nature Reviews Cancer **15**, 730, 2015.
5. E. Stanganello, A. I. H. Hagemann, B. Mattes, C. Sinner, D. Meyen, S. Weber, A. Schug, E. Raz, and S. Scholpp, *Filopodia-based Wnt transport during vertebrate tissue patterning*, Nature communications **6**, 5846, 2015.
6. B. Mattes, Y. Dang, G. Greicius, L. T. Kaufmann, B. Prunsche, J. Rosenbauer, J. Stegmaier, R. Mikut, S. Özbek, G. U. Nienhaus *et al.*, *Wnt/PCP controls spreading of Wnt/β-catenin signals by cytonemes in vertebrates*, Elife **7**, e36953, 2018.
7. T. Hirashima, E. G. Rens, and R. M. H. Merks, *Cellular Potts modeling of complex multicellular behaviors in tissue morphogenesis*, Development, growth & differentiation **59**, 329–339, 2017.

8. Z. Wang, J. D. Butner, R. Kerketta, V. Cristini, and T. S. Deisboeck, *Simulating cancer growth with multiscale agent-based modeling*, in Seminars in cancer biology **30**, Elsevier, 70–78, 2015.
9. András Szabó and R. M. H. Merks, *Cellular potts modeling of tumor growth, tumor invasion, and tumor evolution*, Frontiers in oncology **3**, 87, 2013.
10. A. Shirinifard, J. S. Gens, B. L. Zaitlen, N. J. Popławski, M. Swat, and J. A. Glazier, *3D multi-cell simulation of tumor growth and angiogenesis*, PloS one **4**, e7190, 2009.
11. B. M. Rubenstein and L. J. Kaufman, *The role of extracellular matrix in glioma invasion: a cellular Potts model approach*, Biophysical journal **95**, 5661–5680, 2008.
12. B. Waclaw, I. Bozic, M. E. Pittman, R. H. Hruban, B. Vogelstein, and M. A. Nowak, *A spatial model predicts that dispersal and cell turnover limit intratumour heterogeneity*, Nature **525**, 261, 2015.
13. A. Karolak, D. A. Markov, L. J. McCawley, and K. A. Rejniak, *Towards personalized computational oncology: from spatial models of tumour spheroids, to organoids, to tissues*, Journal of The Royal Society Interface **15**, 20170703, 2018.
14. J. M. Girkin and M. Torres Carvalho, *The light-sheet microscopy revolution*, Journal of Optics **20**, 053002, 2018.
15. J. Jonkman and C. M. Brown, *Any way you slice it – a comparison of confocal microscopy techniques*, Journal of biomolecular techniques: JBT **26**, 54, 2015.
16. M. Adli, *The CRISPR tool kit for genome editing and beyond*, Nature communications **9**, 1911, 2018.
17. C. Ounkomol, S. Seshamani, M. M. Maleckar, F. Collman, and G. R. Johnson, *Label-free prediction of three-dimensional fluorescence images from transmitted-light microscopy*, Nature methods **15**, 917, 2018.
18. T.-L. Liu, S. Upadhyayula, D. E. Milkie, V. Singh, K. Wang, I. A. Swinburne, K. R. Mosaliganti, Z. M. Collins, T. W. Hiscock, J. Shea *et al.*, *Observing the cell in its native state: Imaging subcellular dynamics in multicellular organisms*, Science **360**, eaaq1392, 2018.
19. V. Voleti, K. B. Patel, W. Li, C. Perez Campos, S. Bharadwaj, H. Yu, C. Ford, M. J. Casper, R. W. Yan, W. Liang *et al.*, *Real-time volumetric microscopy of in vivo dynamics and large-scale samples with SCAPE 2.0*, Nature methods **16**, 1054–1062, 2019.
20. J. Snoek, O. Rippel, K. Swersky, R. Kiros, N. Satish, N. Sundaram, M. Patwary, Mr. Prabhat, and R. Adams, *Scalable bayesian optimization using deep neural networks*, in International conference on machine learning, 2171–2180, 2015.
21. M. K. Driscoll, E. S. Welf, A. R. Jamieson, K. M. Dean, T. Isogai, R. Fiolka, and G. Danuser, *Robust and automated detection of subcellular morphological motifs in 3D microscopy images*, Nature methods **16**, 1037–1044, 2019.
22. M. Berghoff, I. Kondov, and J. Hötzer, *Massively parallel Stencil Code Solver with Autonomous Adaptive Block Distribution*, IEEE Transactions on Parallel and Distributed Systems **29**, 2282–2296, 2018.
23. M. Berghoff and I. Kondov, *Scalable Global Network Based on Local Non-Collective Communications*, SC Workshop: Latest Advances in Scalable Algorithms for Large-Scale Systems (ScalA'18), 2018.
24. F. Graner and J. A. Glazier, *Simulation of biological cell sorting using a two-dimensional extended Potts model*, Physical Review Letters **69**, 2013, 1992.

25. A. Balter, R. M. H. Merks, N. J. Popławski, M. Swat, and J. A. Glazier, *The glazier-graner-hogeweg model: extensions, future directions, and opportunities for further study*, in Single-Cell-Based Models in Biology and Medicine, A. Anderson and K. Rejniak (Editors), Springer, 151–167, 2007.
26. D. Krause and P. Thörnig, *JURECA: General-purpose supercomputer at Jülich Supercomputing Centre*, Journal of large-scale research facilities **2**, A62, 2016.